Synthesis and Characterization of Poly(glycidyl methacrylate)/Na-Montmorillonite Nanocomposites

Meltem Çelik, Müşerref Önal

Department of Chemistry, Faculty of Science, Ankara University, 06100 Tandoğan, Ankara, Turkey

Received 20 January 2004; accepted 8 May 2004
DOI 10.1002/app.21075
Published online in Wiley InterScience (www.interscience.wiley.com).

ABSTRACT: Poly(glycidyl methacrylate)/Na–montmorillonite nanocomposites were synthesized by free-radical polymerization of glycidyl methacrylate containing dispersed montmorillonite. By changing the concentration of glycidyl methacrylate several polymer–clay nanocomposites were prepared and the resulting nanocomposites were characterized by X-ray diffraction, Fourier transform infrared spectroscopy, scanning electron microscopy, and thermogravimetric analysis. The results indicated that the properties of the composite were significantly improved. The thermogravimetric analysis results revealed that the degradation temperatures of nanocomposites were higher than that of pure polymer and the thermal degradation rates decreased. Examination of these materials by scanning electron microscopy showed that the clay layers are dispersed homogenously in the polymer matrix and the formation of intercalation nanostructure. Furthermore, adsorptive, moisture regain, and water uptake properties of nanocomposites were also investigated. © 2004 Wiley Periodicals, Inc. J Appl Polym Sci 94: 1532–1538, 2004

Key words: poly(glycidyl methacrylate); clay; montmorillonite; nanocomposites; radical polymerization

INTRODUCTION

In recent years, polymer/clay nanocomposites have become increasingly important because they combine the structural, physical, and chemical properties of both clay and polymer. The efficiency of clay modifies many different properties of the polymer, such as sorbancy, ion exchange capabilities, and thermal and solvent resistance. They give improved mechanical properties, gas barrier properties, and decreased flammability relative to simple polymers.[1] The improved composites are widely used in areas such as construction, electronic, consumer products, and transportation.[2] Nanocomposites can exist in two forms. In the first form, polymer chains are intercalated or inserted in the layers of clay. In the second form, clay layers are exfoliated and dispersed in polymer matrix.[3]

The Na–montmorillonite (Na–MMT) clay is one of the widely used structurally layered silicates for this purpose. With only a low content of MMT, improved physical properties of the polymer can be obtained. Also, the hydrophilic nature of the clay surfaces provides homogeneous dispersion in the organic polymer phase.

Glycidyl methacrylate (GMA) is an important vinyl monomer for desirable properties such as high strength and is relatively less toxic, polar, and less expensive than other vinyl monomers. However, some minor qualities such as thermal stability and poor physical performance need to be improved. Poly(glycidyl methacrylate) (PGMA)/MMT nanocomposites offer the potential for excellent thermal properties and enchanced physical performance.

Recently, many polymer/clay nanocomposites have been synthesized, including nylon 6,[4–8] nylon 10,10,[9] polystyrene,[10–15] polypyrrole,[16] polyimide,[17,18] polyacrylate,[19] polyacrylonitrile,[20] etc., but poly(glycidyl methacrylate) seems to have been neglected.

Owing to our interest in developing new materials with improved properties, the purpose of this study was to synthesize poly(glycidyl methacrylate)/Na–montmorillonite nanocomposites by free-radical polymerization. In addition, the effect of monomer concentration on the physical properties of nanocomposites such as adsorption, moisture regain, and water uptake were investigated. Also, the thermal and morphological properties of nanocomposites were characterized.

EXPERIMENTAL

Materials and methods

The montmorillonite used in this study was obtained by the purification of the Reşadiye (Tokat/Turkey) Bentonite. The specific surface area (S_{BET}) of the sample was 43 m^2/g, its cation-exchange capacity (CEC) was 108 mEq/100 g, and the interlayer spacing of this

Correspondence to: M. Çelik (mecelik@science.ankara.edu.tr).

TABLE I
The Compositions of the PGMA/Na–MMT Nanocomposites

Sample	Monomer (GMA)[a] (wt %)	Na-MMT[b] (wt %)	Product[c] (wt %)
PGMA/Na–MMT1	21.18	78.82	82.38
PGMA/Na–MMT2	34.96	65.04	108.14
PGMA/Na–MMT3	44.64	55.36	157.40
PGMA/Na–MMT4	51.81	48.18	165.06
PGMA/Na–MMT5	61.72	38.28	225.10
PGMA/Na–MMT6	68.25	31.75	235.37
PGMA/Na–MMT7	72.88	27.12	301.08
PGMA/Na–MMT8	76.33	23.67	335.89
PGMA/NA–MMT9	79.00	21.00	372.36
PGMA/Na–MMT10	81.13	18.87	434.27

Bz_2O_2 concentration = 3.0×10^{-3} mol/L, temperature = 85°C, time = 2 h.
[a] Calculated by dividing of the weight of monomer by the weight of (clay + monomer).
[b] Calculated by dividing of the weight of clay by the weight of (clay + monomer).
[c] Expressed as (the weight of product/the weight of clay) × 100.

sample was 1.21 nm. The chemical composition of the montmorillonite was 61.97% SiO_2, 19.73% Al_2O_3, 4.74% Fe_2O_3, 0.91% CaO, 2.40% MgO, 2.58% Na_2O, 0.38% K_2O, 0.22% TiO_2, and 7.08% loss on ignition (LOI), which was determined by atomic absorption spectrometry. Reagent grade GMA (Merck) was distilled before use. Benzoyl peroxide (Bz_2O_2) (Merck) was recrystallized twice from a methanol and chloroform mixture. All other chemicals were of chemically pure grade.

Determination of cation-exchange capacity

Cation-exchange capacity, defined as the milliequivalents of exchangeable cations per 100 g (mEq/100 g) of clay or clay minerals was determined by the methylene blue standard procedure.[21–23] The CEC of the Na–MMT used was determined to be 108 mEq/100 g.

Purification of clay

The original bentonite was ground to pass through a 0.074 mm sieve and dried for 4 h at 105°C. A desired amount of original bentonite was purified by decantation and precipitation from its aqueous suspension.[24] Hence, a rather pure Na–MMT was obtained.

Synthesis of PGMA/clay nanocomposites

The nanocomposites were synthesized according to the following procedure. A suspension of Na–MMT (1.00 ± 0.01 g) in 29 mL distilled water was stirred overnight, and then a suitable concentration of GMA and Bz_2O_2 as radical initiator (dissolved in 1 mL acetone) was added to it. The mixture was mixed vigorously. The stirred mixture was then placed in a water bath (Lauda D40 S, Germany) adjusted to the polymerization temperature (85°C) for 2 h. At the end of polymerization, the polymerization tube was taken from the water bath and the suspended product was separated by centrifugation. The crude product was washed several times with distilled water and extracted with acetone in a Soxhlet for 2 h to remove the unreacted monomer. The obtained nanocomposites were dried at 40°C under vacuum and then weighed. The other samples were prepared by the same procedure using different concentrations of GMA. Table I shows the mixing weight ratio of samples and the polymerization conditions.

Characterization of PGMA/clay nanocomposites

FTIR spectra

FTIR spectra of the samples were recorded on a MATTSON 1000 Model FTIR spectrophotometer.

X-ray diffraction

XRD analysis was performed by a Rikagu D-max 2200 X-ray diffractometer, using CuKα X-rays whose wavelength was 1.5418 nm, and a Ni filter was used.

Thermogravimetric analysis

The thermogravimetric measurements were performed on a Rheometric Scientific 1000+ Model thermal analyzer under nitrogen atmosphere with a flow rate of 200 mL/min and a heating rate of 10°C/min. The temperature range expanded from room temperature to 600°C.

Scanning electron microscopy

The surface morphology of nanocomposites was examined by means of a JEOL-JEM 100 CX II Model scanning electron microscope, after gold coating.

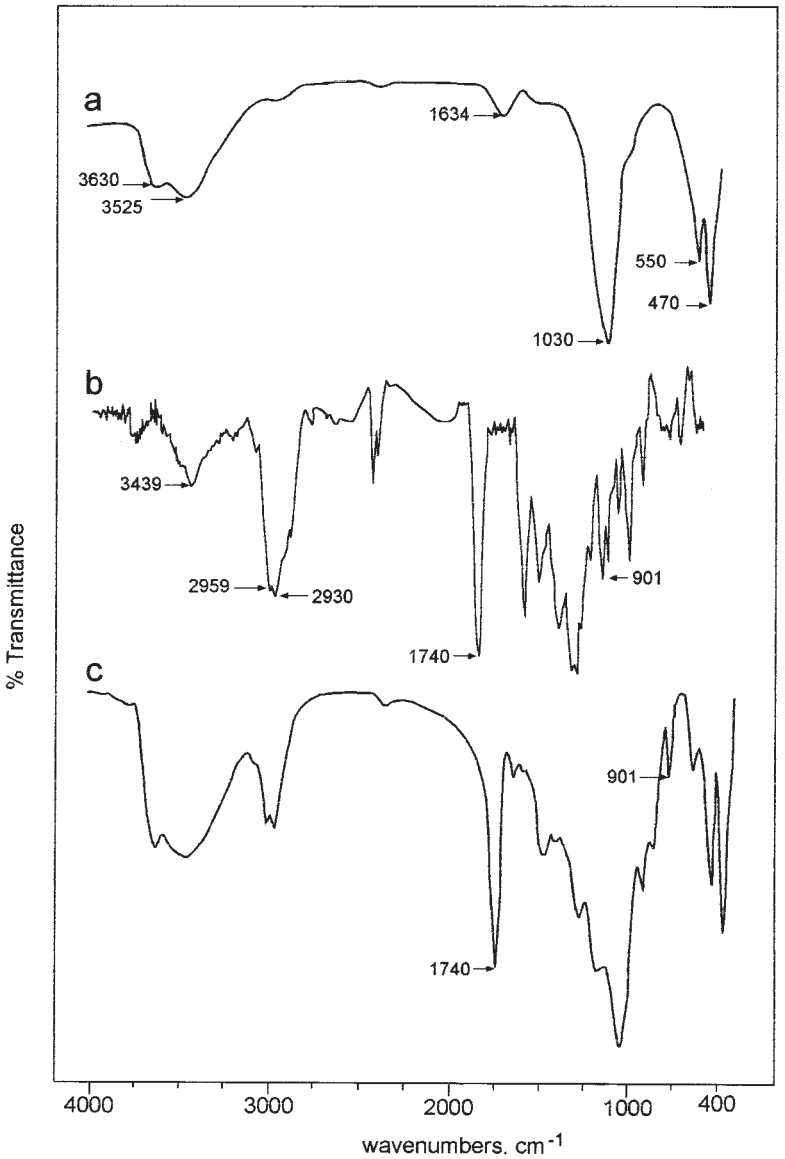

Figure 1 The FTIR spectra of (a) pure Na–MMT, (b) pure PGMA, and (c) PGMA/Na–MMT5 (61.72 wt % GMA).

Adsorptive properties

The adsorption and desorption isotherms at liquid nitrogen temperature of samples were also determined. A volumetric adsorption instrument fully constructed of Pyrex glass and connected to high vacuum was used in the experiments.[25]

Moisture regain

The weighed dry samples were placed in a desiccator over water (100% humidity) and kept at 25°C for 72 h, closing the cap of the desiccator. The moisture regain values of samples were calculated from their dry and conditioned weights (i.e., moisture regain = $(W_2 - W_1)/W_1 \times 100$, where W_1 and W_2 are the weights of the dry and wet samples, respectively).[26]

Water uptake

The dry samples were weighed and kept in water for 2 h at 25°C. The wet weights were determined after sandwiching the samples between the filter paper 10 times. The water uptake of samples was determined from water uptake = $(W_2 - W_1)/W_1 \times 100$, where W_1 and W_2 are the weights of the dry and wet samples, respectively.[26]

RESULTS AND DISCUSSION

Nanocomposites were characterized by using Fourier transform infrared spectroscopy, X-ray diffraction, scanning electron microscopy, and thermogravimetric analysis.

Figures 1(a)–(c) gives the FTIR spectra of pure Na–MMT, pure PGMA, and PGMA/Na–MMT nanocomposite containing 61.72 wt % GMA monomer, respec-

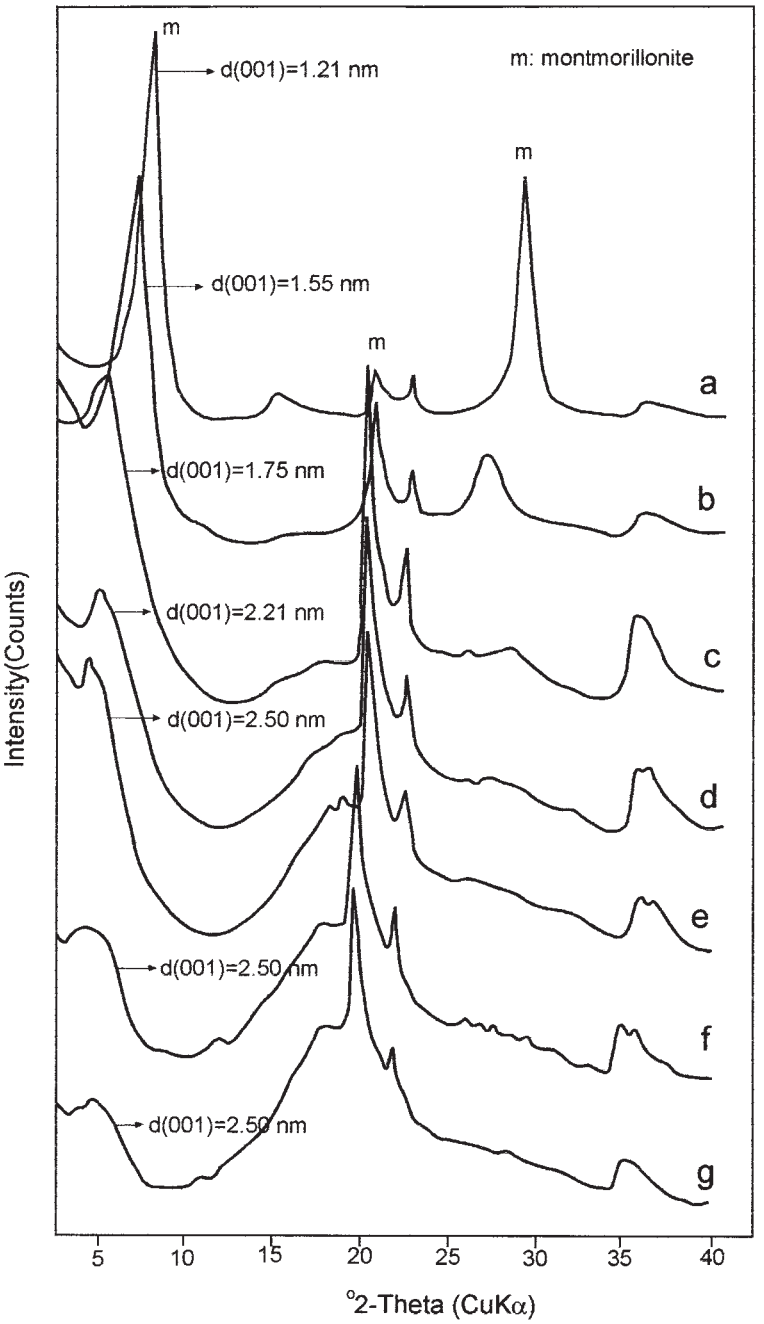

Figure 2 XRD patterns of pure Na–MMT and PGMA/Na–MMT nanocomposites with different GMA contents: (a) pure Na–MMT, (b) PGMA/Na–MMT1 (21.18 wt % GMA), (c) PGMA/Na–MMT2 (34.96 wt % GMA), (d) PGMA/Na–MMT5 (61.72 wt % GMA), (e) PGMA/Na–MMT6 (68.25 wt % GMA), (f) PGMA/Na–MMT7 (72.88 wt % GMA), (g) PGMA/Na–MMT10 (81.13 wt % GMA).

tively. In the spectrum of pure Na–MMT the band at 470 cm^{-1} is a Si–O–Si deformation band, the band at 550 cm^{-1} is a Si–O–Al deformation band, the band at 1,030 cm^{-1} is a Si–O stretching band, the band at 1,634 cm^{-1} is an O–H deformation band of H_2O, the band at 3,525 cm^{-1} is an O–H in stretching band of H_2O, and the band at 3,630 cm^{-1} is an O–H stretching band of the inner surfaces of clay. The spectrum of pure PGMA shows the characteristic stretching vibration band of bound hydrogen at 3,439 cm^{-1} and the peaks at 2,959 and 2,930 cm^{-1} are attributed to the C–H stretching of methylene and methyl groups of PGMA. PGMA/Na–MMT nanocomposite containing 61.72 wt % GMA monomer spectrum also shows the bands at 1,740 and 901 cm^{-1} coming from the carbonyl group and the epoxy groups of PGMA, which is not found in the FTIR spectrum of the pure Na–MMT. This means that the PGMA has been intercalated into the sheets of Na–MMT.

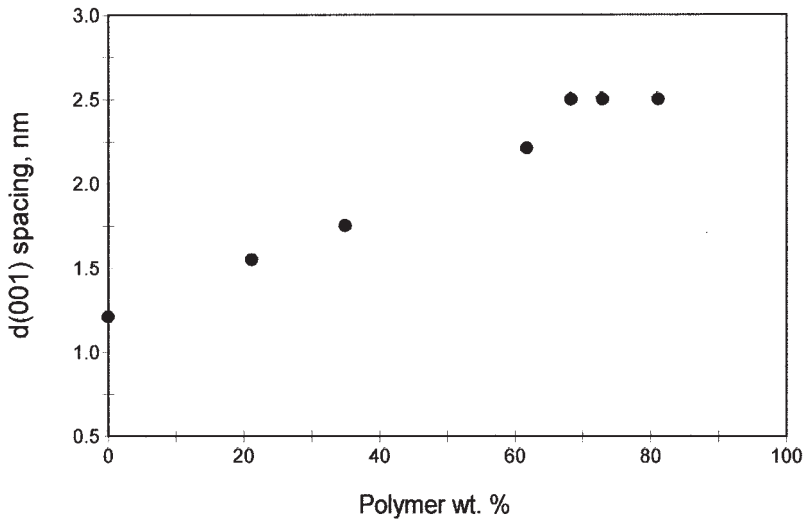

Figure 3 Basal spacing of Na–MMT as a function of PGMA weight percent.

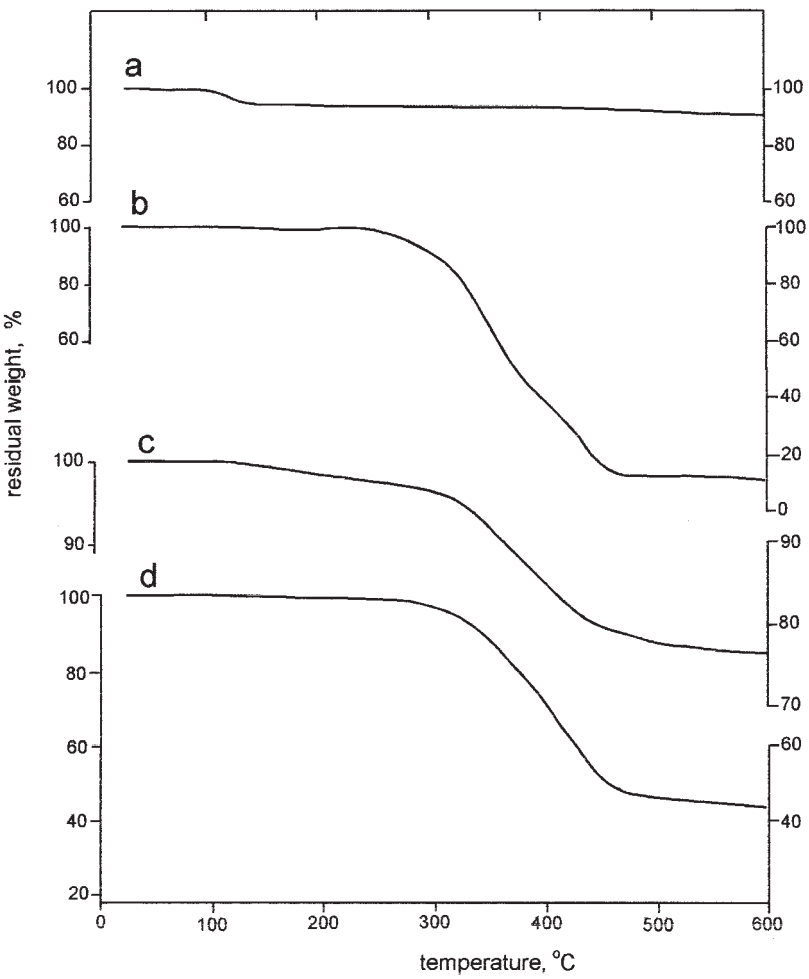

Figure 4 TGA curves of (a) pure Na–MMT, (b) pure PGMA, (c) PGMA/Na–MMT2 (34.96 wt % GMA), and (d) PGMA/Na–MMT5 (61.72 wt % GMA) obtained in nitrogen atmosphere at heating rate of 10°C/min.

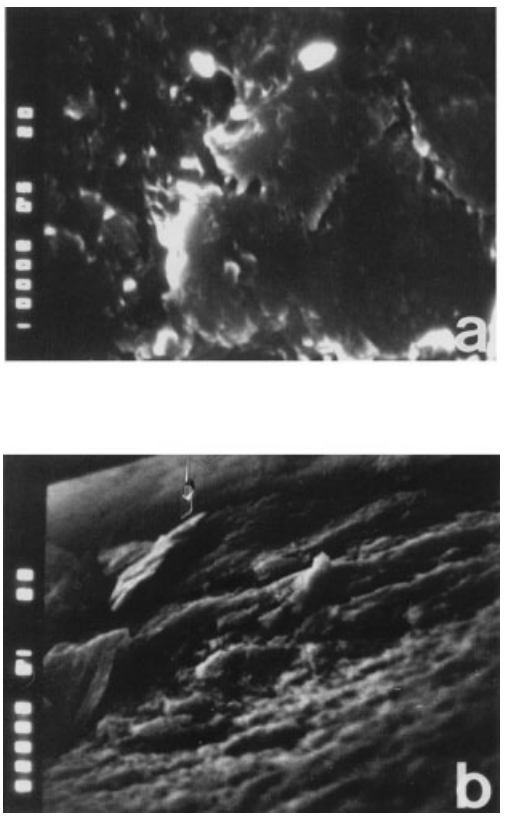

Figure 5 SEM micrographs of (a) pure Na–MMT at a magnification of ×5000 and (b) PGMA/Na–MMT5 (61.72 wt % GMA) at a magnification of ×1500.

Further evidence for the intercalation can be obtained by XRD. The XRD patterns of the pure Na–MMT and nanocomposites with different GMA monomer contents are shown in Figures 2 (a)—(g). The interlayer spacing (d_{001}) values of the pure Na–MMT and the samples were calculated according to Bragg's equation, $d = \lambda/2\sin\theta$. The obtained results are presented in Figure 3. Figures 2 and 3 showed that the diffraction pattern of the (d_{001}) spacing of pure Na–MMT was 1.21 nm and, after intercalation polymerization, the diffraction patterns of PGMA/Na–MMT nanocomposites were higher with the increase of the GMA monomer content (from 21.18 to 68.25 wt %). For PGMA/Na–MMT nanocomposites containing 68.25 wt % GMA monomer, the strong peak corresponding to (d_{001}) spacing at 2.50 nm was clearly observed and no further increase of interlayer distance at higher glycidyl methacrylate content was observed. These results indicate that the PGMA molecules penetrate through the interlayer and expand the interlayer spacing. In other words, PGMA monomer can polymerize to form intercalated and partially exfoliated nanocomposites.

The TGA thermograms of pure Na–MMT, pure PGMA, and PGMA/Na–MMT nanocomposites are shown in Figure 4. Evidently, PGMA/Na–MMT nanocomposite containing 34.96 wt % GMA monomer has a higher decomposition temperature than pure PGMA, and this indicates the enhancement of the thermal stability of PGMA by adding montmorillonite into the PGMA matrix. A possible reason is that Na–MMT is an inorganic material with high thermal stability and great barrier properties that can prevent the heat from transmitting quickly and can limit the continuous decomposition of the nanocomposites, but with the GMA content further increased to 61.72 wt %, has a lower decomposition temperature than 34.96 wt % GMA containing nanocomposite because the clay content is low in this sample. The TGA curve of pure Na–MMT indicates that there are two stages of decomposition. The first one is small and due to the loss of absorbed water when the temperature is lower than 250°C. At 600°C, the weight loss of the Na–MMT reaches about 6.76%. As shown in Figure 4, the decomposition temperature of the pure PGMA is 260.55°C; its weight loss reaches 94.33% at 600°C. In contrast, the weight loss of the PGMA/Na–MMT nanocomposite containing 34.96 wt % GMA monomer started at 297.06°C and reached a value of 25% at 600°C. This indicates that the thermal stability of the PGMA/Na–MMT nanocomposite is quite remarkable. As a result the improvement in thermal stability of the composite is mainly attributed to thermal resistance of Na–MMT and nanodispersion of Na–MMT sheets in the PGMA matrix. And, finally, intercalation with Na–MMT could notably improve thermal stability of PGMA.

Scanning electron microscopy is a very useful tool for characterizing the structure of polymer/clay nanocomposites. SEM was used to observe the morphology of the pure Na–MMT and PGMA/Na–MMT nanocomposite containing 61.72 wt % GMA monomer as illustrated in Figures 5 (a) and (b). Examination of the PGMA/Na–MMT nanocomposite by scanning electron microscopy has shown the effect of PGMA composition on the morphology of MMT material and the interlayer spacing of Na–MMT is expanded [Fig. 5(b)]. From Figure 5(b), the intercalated morphology can be seen.

Properties of PGMA/clay nanocomposites

Adsorptive properties

The specific surface areas (S_{BET}) of pure Na–MMT and nanocomposites were determined by the Brunauer–Emmett–Teller procedure by using N_2 adsorption data.[27] The specific micromesopore volumes (V) were calculated from the desorption data.[28] While the specific surface area and micromesopore volumes of pure Na–MMT were 43 m^2g^{-1} and 0.065 cm^3g^{-1}, respectively, these values drastically decreased to 6 m^2g^{-1} and 0.006 cm^3g^{-1} for PGMA/Na–MMT containing 51.81 wt % GMA, respectively. It was observed that, for higher loading of PGMA, the specific surface area and micromesopore volumes of nanocomposites notably decreased and

TABLE II
The Moisture Regain and Water Uptake Values of Pure Na–MMT and PGMA/Na–MMT Nanocomposites

Sample	Moisture regain (%)	Water uptake (%)
Pure Na–MMT	23.38	297.34
PGMA/Na–MMT1	22.20	274.54
PGMA/Na–MMT2	18.93	133.20
PGMA/Na–MMT3	15.70	64.48
PGMA/Na–MMT4	14.70	43.93
PGMA/Na–MMT5	10.32	35.27
PGMA/Na–MMT6	10.00	33.08
PGMA/Na–MMT7	9.84	32.16
PGMA/Na–MMT8	9.80	25.82
PGMA/Na–MMT9	9.00	23.06
PGMA/Na–MMT10	8.48	22.82

Bz_2O_2 concentration = 3.0×10^{-3} mol/L, temperature = 85°C, time = 2 h.

nearly approached zero. This could be explained in terms of covering or filling of the pores by PGMA.

Moisture regain and water uptake measurements

The moisture regain and water uptake values of pure Na–MMT and PGMA/Na–MMT nanocomposites are listed in Table II. It was observed that the moisture regain and water uptake values of the nanocomposites were decreased.

The decrease in moisture regain, which is a desirable property, can be attributed to the hydrophobic character of the PGMA and the hydrophilicity of Na–MMT has been changed to an organophilic nature. The decrease in water uptake can be explained by the fact that the percentage of clay in the composites is limited, which reflects that the quantity of the polymer introduced in the layers reaches a limit and is enough to achieve maximum opening of the interlayers of clay[29] and the formation of a crosslinked structure to a certain extent that prevents the insert on of water molecules into the structure.[26] Finally, water resistance of these composites can be greatly improved. This means the material has more stable properties, which is interesting for practical applications.[30]

CONCLUSION

Poly(glycidyl methacrylate)/Na–MMT nanocomposites have been successfully prepared by free-radical polymerization, and its thermal as well as physical properties were investigated. XRD results reveal that intercalated and partially exfoliated structures have been obtained and increased intercalation with increasing amount of the polymer. Interlayer distance of Na–MMT increased with glycidyl methacrylate content up to 68.25 wt % and no further increase of interlayer distance at higher glycidyl methacrylate content was observed. Thermogravimetric analysis results showed that these nanocomposites exhibited better thermal stability than pure poly(glycidyl methacrylate). In addition, the physical properties of nanocomposites have also been determined. Adsorptive, moisture regain, and water uptake properties of composites obviously decreased compared with that of pure Na–MMT. A significant decrease in these parameters with monomer concentration was observed.

The authors thank Ankara University Research Fund (Project Number 20040705087) and the Turkish Scientific and Research Institute by project TBAG-1986(100T101) for their financial support to this work.

References

1. Li, Y.; Zhao, B.; Xie, S.; Zhang, S. Polym Int 2003, 52, 892.
2. Salahuddin, N.; Akelah, A. Polym Adv Technol 2002, 13, 339.
3. Zhu, J.; Wilkie, C. A. Polym Int 2000, 49, 1158.
4. Liu, X.; Wu, Q.; Berglund, L. A.; Qi, Z. Macromol Mater Eng 2002, 287, 515.
5. Kojima, Y.; Usuki, A.; Kawasumi, M.; Okada, A.; Kurauchi, T.; Kamigaito, O. J Polym Sci Part A: Polym Chem 1993, 31, 983.
6. Ma, C. M.; Kuo, C.; Kuan, H.; Chiang, C. J Appl Polym Sci 2003, 88, 1686.
7. Kojima, Y.; Usuki, A.; Kawasumi, M.; Okada, A.; Kurauchi, T.; Kamigaito, O. J Appl Polym Sci 1993, 49, 1259.
8. Kyu, T.; Zhou, Z. L.; Zhu, G. C.; Tajuddin, Y.; Qutubuddin, S. J Polym Sci Part B: Polym Phys 1996, 34, 1761.
9. Zhang, G.; Yan, D. J Appl Polym Sci 2003, 88, 2181.
10. Hasegawa, N.; Okamoto, H.; Kawasumi, M.; Usuki A. J Appl Polym Sci 1999, 74, 3359.
11. Moet, A.; Akelah, A. Mater Lett 1993, 18, 97.
12. Chen, G.; Liu, S.; Chen S.; Qi, Z. Macromol Chem Phys 2001, 202, 1189.
13. Tseng, C.; Wu, J.; Lee, H.; Chang, F. J Appl Polym Sci 2002, 85, 1370.
14. Kato, C.; Kuroda, K.; Takahara, H. Clays Clay Miner 1981, 29, 294.
15. Moet, A.; Akelah, A. J Mater Sci 1996, 28, 3589.
16. Yeh, J.; Chin, C.; Chang, S. J Appl Polym Sci 2003, 88, 3264.
17. Yano, K.; Usuki, A.; Okada, A.; Kurauchi, T.; Kamigaito, O. J Polym Sci Part A: Polym Chem 1993, 31, 2493.
18. Yano, K.; Usuki, A.; Okada, A. J Polym Sci Part A: Polym Chem 1997, 35, 2289.
19. Chen, Z.; Huang, C.; Liu, S.; Zhang, Y.; Gong, K. J Appl Polym Sci 2000, 75, 796.
20. Seçkin, T.; Gültek, A.; İçduygu, M. G.; Önal, Y. J Appl Polym Sci 2002, 84, 164.
21. Hang, P. T.; Brindley, G. W. Clays Clay Miner 1970, 18, 203.
22. Rytwo, G.; Serben, C.; Nir, S.; Margulies, L. Clays Clay Miner 1991, 39, 551.
23. Sarıkaya, Y.; Önal, M.; Baran, B.; Alemdaroğlu, T. Clays Clay Miner 2000, 48, 557.
24. Önal, M.; Sarıkaya, Y.; Alemdaroğlu, T.; Bozdoğan, İ. Turk J Chem 2003, 27, 683.
25. Önal, M.; Sarıkaya, Y.; Alemdaroğlu, T. Turk J Chem 2001, 25, 241.
26. Keleş, H.; Çelik, M.; Saçak, M.; Aksu, L. J Appl Polym Sci 1999, 74, 1547.
27. Brunauer, S.; Emmett, P. H.; Teller, E. J. J Am Chem Soc 1938, 60, 309.
28. Sarıkaya, Y.; Alemdaroğlu, T.; Önal, M. J Eur Ceram Soc 2002, 22, 305.
29. Salahuddin, N.; Rehab, A. Polym Int 2003, 52, 241.
30. Han, B.; Cheng, A.; Ji, G.; Wu, S.; Shen, J. J Appl Polym Sci 2004, 91, 2536.